X-Ray Spectroscopy of Hydrogen-Like Ions in an Electron Beam Ion Trap

M.R.Tarbutt[1], D.Crosby[1], E.G.Myers[2], N.Nakamura[3], S.Ohtani[3], and J.D.Silver[1]

[1] University of Oxford, Clarendon Laboratory, Parks Road, Oxford, OX1 3PU, UK
[2] Department of Physics, Florida State University, Tallahassee, FL 32306, USA
[3] Cold Trapped Ions Project, ICORP, JST, 1-40-2 Fuda, Chofu, Tokyo 182-0024, Japan

Abstract. The X-ray emission from highly charged hydrogen-like ions in an electron beam ion trap is free from the problems of satellite contamination and Doppler shifts inherent in fast-beam sources. This is a favourable situation for the measurement of ground-state Lamb shifts in these ions. We present recent progress toward this goal, and discuss a method whereby wavelength comparison between transitions in hydrogen-like ions of different nuclear charge Z, enable the measurement of QED effects without requiring an absolute calibration.

1 Introduction

The $1s$ Lamb shift in highly charged one-electron ions tests QED theory in a strong-field regime. There has recently been much theoretical interest in the two-loop self energy contribution to the Lamb shift, which can be written as a series expansion in $(Z\alpha)$ [1]:

$$E(\text{2-loop}) = \left(\frac{\alpha}{\pi}\right)^2 \frac{(Z\alpha)^4}{n^3} m_e c^2 [B_{40} + (Z\alpha)B_{50} + ...]. \quad (1)$$

It has been noted that the coefficient B_{50}, evaluated as -21.6 [1,2], is suprisingly large, while Mallampalli and Sapirstein have questioned the validity of a perturbative approach for the evaluation of the 2-loop self energy, even at low Z [3]. Moreover, the results of Goidenko et al. [4], for the loop after loop contribution to the second order self energy are in strong disagreement with the calculation of Mallampalli and Sapirstein [3]. While Lamb shift measurements in atomic hydrogen are sufficiently precise to test the 2-loop self energy contribution, the interpretation of the measurements is obscured by the uncertainty in the finite size of the proton. This problem may be removed in the future through a measurement of the Lamb shift in muonic hydrogen [5]. In hydrogen-like ions, measurements of the $1s$ Lamb shifts are not yet sufficiently precise to test the theory at the level of the 2-loop self energy. The current situation is summarised in Fig.1, which shows the complete $1s$ Lamb shift (including the nuclear size corrections) [6], the contribution from the nuclear size correction to the Dirac energy (as given in [6]), and the value of the term $(\alpha/\pi)^2(Z\alpha)^5 B_{50} m_e c^2$ in (1).

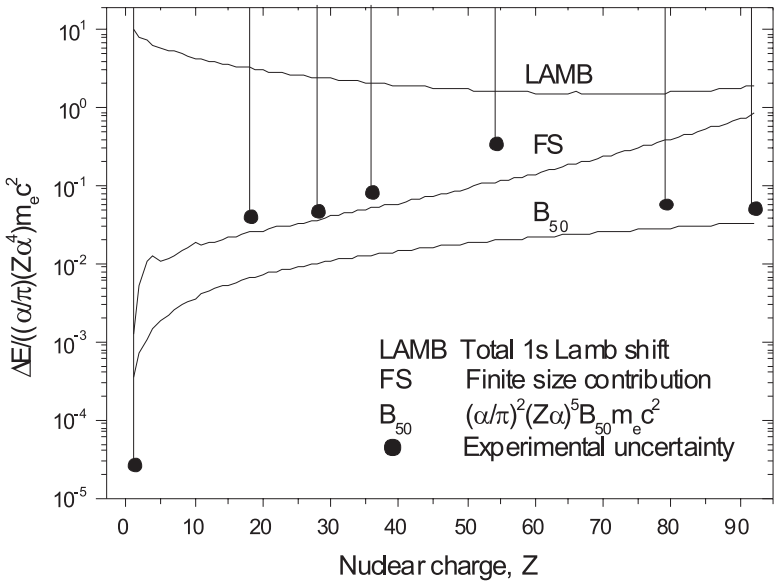

Fig. 1. 1s Lamb shift, contributions from nuclear size and binding corrections to the two-loop self energy. Experimental uncertainties are shown for specific values of Z, with references given in the text

All are shown in units of $(\alpha/\pi)(Z\alpha)^4 m_e c^2$. For specific values of Z the uncertainties in the experimental values for the 1s Lamb shift are shown: Z=1: [7], Z=18: [8], Z=28: [9], Z=36: [10], Z=54: [11], Z=79: [12], Z=92: [13]. With the exception of hydrogen, the experimental uncertainties are considerably larger than the theoretical ones.

The most precise 1s Lamb shift measurements in the hydrogen-like ions have been performed using fast beams of foil-stripped ions, and X-ray spectroscopic comparison against X-ray wavelength standards. At high Z the two Lyman-α components can be resolved using germanium solid state detectors of high efficiency. In the measurements of Au^{78+} and U^{91+}, the Lyman-α lines were Doppler shifted to be nearly coincident with suitable γ-ray standards. For the medium Z measurements, the Kα wavelengths of the neutral elements serve to calibrate. In all these experiments, the precision was limited by spectator-electron satellite contamination, Doppler shift uncertainties and counting statistics.

In this paper, we summarise our progress towards 1s Lamb shift measurements on medium Z hydrogen-like ions produced in an electron beam ion trap (EBIT), where the X-ray emission is free from the problems of satellite contamination and Doppler shifts. In this context, we note that a measurement of the 1s Lamb shift in hydrogen-like Mg^{11+} has been performed at the Livermore EBIT using a quasimonolithic crystal setup, and reaching a precision of 13% for the Lamb shift dominated by counting statistics [14]. With our setup, the

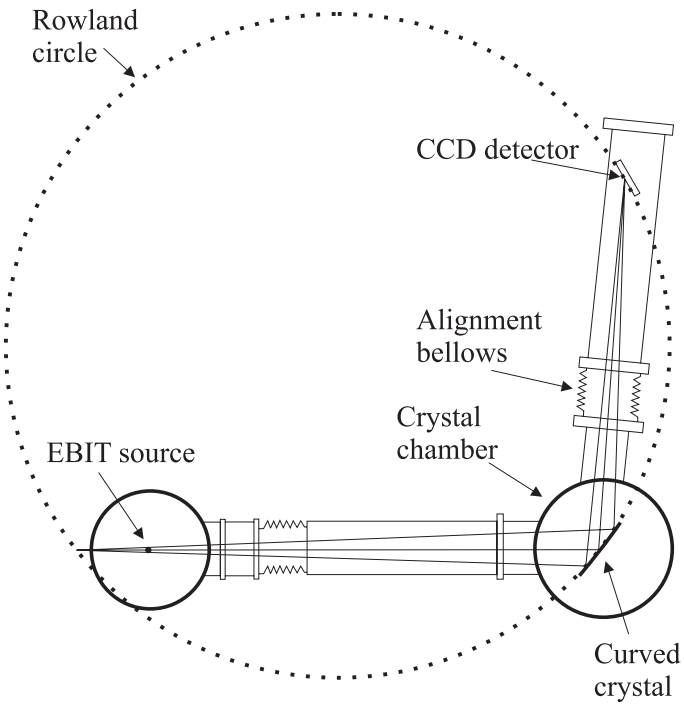

Fig. 2. Johann geometry crystal spectrometer coupled to the Oxford EBIT. Not to scale

counting statistics are very much higher, and the difficulty is one of calibration. We consider two calibration methods, the traditional method of using the known Kα wavelengths, and a new method which avoids the use of external calibration lines altogether.

2 Experiment Setup

Our experimental setup consists of a Johann-type X-ray spectrometer [15] coupled to the Oxford electron beam ion trap [16], as shown in Fig.2.

2.1 Electron Beam Ion Traps

An EBIT is a device for producing, trapping and exciting highly charged ions, as has been described in detail elsewhere, e.g. [17]. Inside the EBIT trapping region, a nearly monoenergetic electron beam is compressed to a high current density by an axial magnetic field. Neutrals, or low charge state ions are injected into the trap where they are ionized to high charge states and excited by electron impact. These ions are confined radially by the magnetic field and the space charge of the electron beam, and are confined axially by the application of an electrostatic

potential well $V_{\rm ax}$. For the purposes of this paper, the EBIT is a highly charged ion X-ray source, and the important parameters are the spatial dimensions and temperature of the X-ray emitting ion cloud. The source is a cylinder, defined radially by the extent of the electron beam, diameter ≈ 70 μm, and axially by the extent of the potential well, length $\approx$25 mm. Ions of charge q are heated mainly by elastic collisions with the beam electrons, and in the absence of any cooling mechanism would reach the temperature required for axial escape from the trap, $k_BT = qV_{\rm ax}$. However, an evaporative cooling mechanism operates whereby the highly charged ions exchange energy with ions of low charge state q' for which the axial escape temperature is lower by a factor q'/q. It is therefore common to simultaneously inject into the trap a light 'coolant' gas, along with the element of interest. Typical source temperatures are in the region of 500-1000 eV, although under suitable conditions, temperatures as low as 60 eV have been demonstrated [18].

2.2 High Resolution X-ray Spectroscopy

To obtain X-ray spectra of high resolution, a crystal spectrometer is required. Although flat crystal spectrometers have been used successfully for EBIT X-ray spectroscopy e.g [19], their efficiency is low because the crystal reflectivity is only high inside a very small angular range about the Bragg angle, $\theta_{\rm B}$. To improve the efficiency, the crystal can be curved in such a way that the Bragg condition is met over a large portion of the crystal surface. In our spectrometer, a 4-bar bender is used to curve the crystal in the plane of dispersion with a cylindrical curvature of radius R, where R is the *diameter* of an imaginary circle, the Rowland circle (see Fig.2). If both crystal and detector are placed on the Rowland circle, a distance $R\sin\theta_{\rm B}$ apart, X-rays of a given wavelength are brought to a focus at the detector. The detector is a low noise, liquid nitrogen cooled X-ray CCD, with 1152 x 1242 pixels and 22.5 μm spatial resolution. Provided that each pixel contains only a single X-ray photon, there is energy resolution of 150 eV in every pixel, allowing signal X-rays to be well discriminated from the background. The crystal and detector are mounted on a common rigid arm in order to minimize motion-related line shifts. The spectrometer is operated in vacuum, with the ultra-high vacuum of the EBIT separated from the low vacuum of the spectrometer by a 25 μm beryllium window. The source is placed on or inside the Rowland circle, with the source axis perpendicular to the plane of dispersion. If the source is placed on the Rowland circle, the Bragg condition is met (for a given wavelength) over a large portion of the crystal and the spectrometer is maximally efficient. Conversely, the Bragg condition can then only be met for a small range of wavelengths so that the 'bandwidth' of the spectrometer is small. As the source is moved inside the Rowland circle, the efficiency for a given wavelength decreases, while the range of reflected wavelengths (the bandwidth) increases. For a given experiment, the source position is therefore chosen to give the maximum possible efficiency consistent with the required bandwidth.

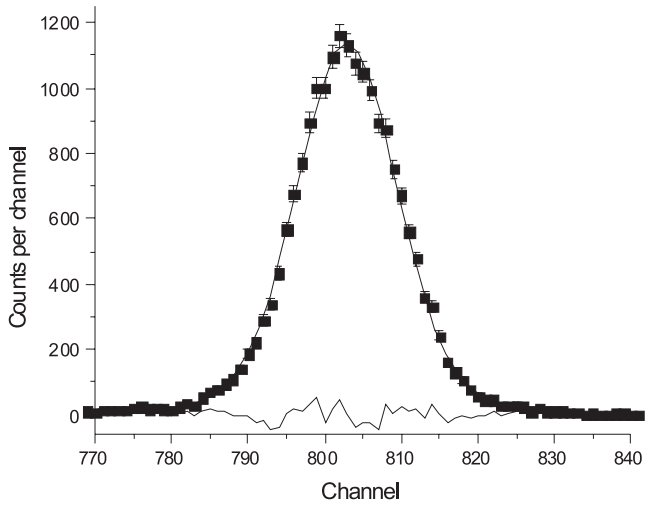

Fig. 3. Ar^{17+} $2p_{3/2} - 1s_{1/2}$

3 Recent Results

3.1 Lineshape Studies of Ar^{17+} Lyman-α

In figure 3 we show an example spectrum of the hydrogen-like Ar^{17+} $2p_{3/2}-1s_{1/2}$ line at 3.3 keV recorded using the experimental setup described above. Here, we used a Si(111) crystal with a radius of curvature $R = 1357\,\mathrm{mm}$ and the source placed very close to the Rowland circle for high efficiency. The electron beam energy was 7 keV and the beam current 120 mA, and the accumulation time for this data was 2 hours. The resolution of this spectrum is $\Delta\lambda/\lambda \approx 1/3000$, whereas the intrinsic resolving power of the crystal is 7500. The ion temperature makes a large contribution to the observed linewidth. At a temperature T ions of mass M have a Doppler width given by

$$\left(\frac{\Delta\lambda}{\lambda}\right)_{\mathrm{Dopp}} = \sqrt{\frac{8T\ln 2}{Mc^2}}, \tag{2}$$

so a temperature of 300 eV implies $(\Delta\lambda/\lambda)_{\mathrm{Dopp}} \approx 1/5000$. Voigt fits to our datasets are dominated by the Gaussian component, and clear evidence for Doppler broadening has been obtained by lowering the axial trapping potential V_{ax} thereby lowering the ion temperature. Figure 4 shows the resulting linewidths as a function of the applied axial trapping potential. Crystal imperfections and imperfect focussing may also contribute to the linewidth, while broadening due to the finite dimensions of the source are not significant here.

In figure 3 a voigt fit is shown to guide the eye, while a complete lineshape model will be constructed using a code which ray-traces and solves the equations of dynamical diffraction inside the crystal [20]. Importantly, the line shows

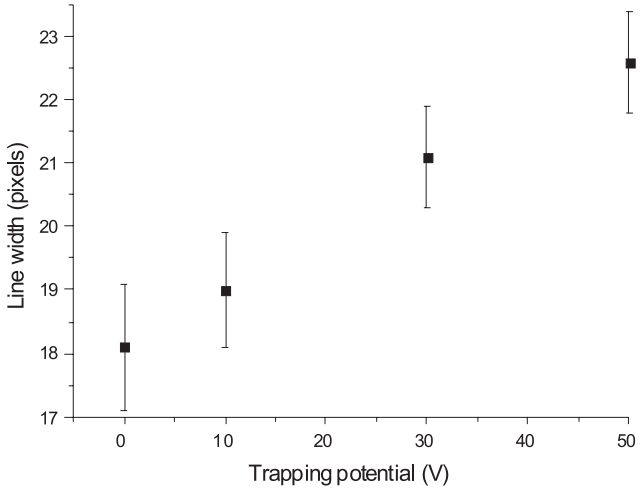

Fig. 4. Linewidths as a function of the axial trapping potential in the EBIT

no evidence of contamination by spectator electron satellite transitions, a problem which limits the obtainable accuracy of similar spectroscopy on fast beam sources, and particularly on recoil ion sources, as in [8]. The absence of satellite contamination is due to the excitation conditions inside the EBIT, where double excitation is rare because the decay processes are faster than the excitation processes, and the electron beam energy is tuned away from dielectronic resonances. We note that although this spectrum is uncalibrated, the resolution and statistics are sufficient to locate the line centroid with a precision of $\Delta\lambda/\lambda = 10^{-6}$, i.e. if the spectrum could be accurately calibrated, the precision would be 3.3 meV (the current uncertainty in the value for this wavelength is 16 meV).

3.2 Ti^{21+} Lyman-α and Vanadium Kα

We have recently obtained the spectrum of hydrogen-like Ti^{21+} Lyman-α on a common scale with the Kα lines of neutral Vanadium, as shown in figure 5. As pointed out above, the Kα lines of the transition elements are the wavelength standards in the X-ray region, and have been used to calibrate previous measurements of Lyman-α in the medium-Z hydrogen-like ions. In this experiment, we placed the EBIT source inside the Rowland circle to give the required wavelength range. The Ti^{21+} Lyman-α data was obtained using an electron beam energy of 13 keV and current 120 mA. The resolution is $\Delta\lambda/\lambda = 1/3700$, and the statistics during this 7 hour integration time enable a line centroid determination of 2 parts per million. To obtain the spectrum of Vanadium Kα, a 1 mm diameter Vanadium wire probe was inserted into the EBIT trapping region so that the electron beam grazed the tip of the wire. A large flux of characteristic X-rays were then observed from the probe, although the flow of the electron beam through the trapping region and on towards the collector was virtually unaffected. The V Kα spectrum shown in the figure was obtained in 10 minutes

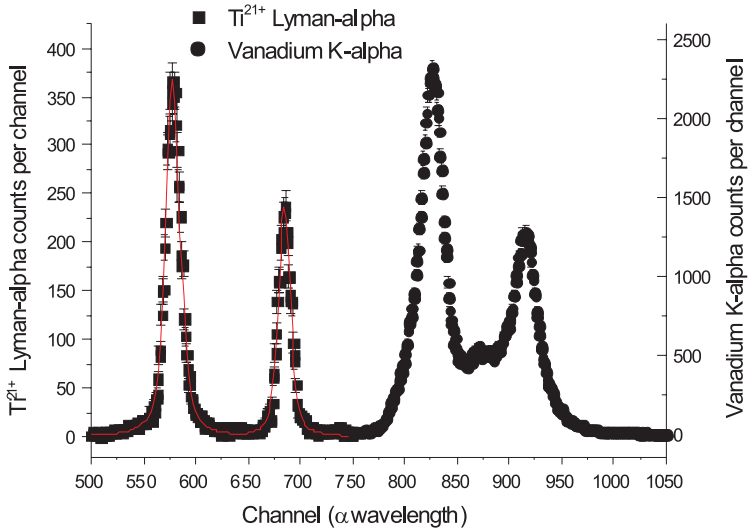

Fig. 5. Ti^{21+} Lyman-α from EBIT and V Kα from wire probe on a common wavelength scale

of integration time. The linewidth is typical for the characteristic X-rays, and the lineshape arises due to multielectronic satellite transitions. Since the calibration X-rays are produced inside the EBIT at the same spatial location as the highly charged ions, systematic shifts due to differences in source locations are minimized. However, the lineshape of the characteristic X-rays produced in this way is different to that produced by a standard X-ray source, as one might expect since the excitation conditions are different in the two cases. For this reason, the probe X-rays do not serve to directly calibrate the Ti^{21+} Lyman-α lines.

4 Future Directions

4.1 Relative and Absolute Wavelength Measurements

We have shown that high resolution X-ray spectra of medium Z hydrogen-like ions can be obtained with a statistical precision of 1 part per million using an EBIT and a Johann curved crystal spectrometer in a relatively short integration time. The calibration of such a spectrum at the same level of precision is problematic. We plan to use a standard X-ray source outside the EBIT to produce the Kα spectrum, and to define the path through the EBIT using a slit which can be centred on the electron beam. To determine the Lyman-α wavelengths from the Kα wavelengths, the dispersion function of the instrument is required. This is strongly constrained by the two known intervals in the spectrum, the Lyman-$\alpha_{1,2}$ interval and the K$\alpha_{1,2}$ interval. In addition, the dispersion function and instrumental profile will be modelled, as for example in [21]. With the development of more intense sources of highly charged ions, such as the new EBIT in

Freiburg [22] and an electron-cyclotron-resonance ion trap (ECRIT) [23], it may soon be possible to make absolute wavelength measurements of the Lyman-α transitions in hydrogen-like ions, using flat or double flat crystal spectrometers.

4.2 An Intercomparison Technique

As we have seen, the wavelength standards in the X-ray region are not ideal calibration standards. They are broad and asymmetric due to the multielectronic satellite transitions, and the line profiles depend on the exact nature of the excitation conditions inside the source. We therefore propose a measurement technique which is sensitive to QED effects in the ground state of hydrogen-like ions, but avoids the use of secondary calibration lines, and does not require the measurement of an absolute wavelength, but rather of a small wavelength difference. We find transitions in two separate hydrogenic ions whose wavelength separation is small.

To illustrate we concentrate on one example, the transitions $2p_{1/2,3/2} - 1s_{1/2}$ in the hydrogen-like ion Mn^{24+} and $3p_{1/2,3/2} - 1s_{1/2}$ in the hydrogen-like ion V^{22+}. The transitions all occur around 6.4 keV, and are very close in energy as shown in figure 6 which is a simulation of the lines expected in such a measurement. The near coincidence occurs because the Dirac contributions to the transition energies:

$$E(n,k,Z) = \left(1 + \left[\frac{Z\alpha}{n - k + (k^2 - Z^2\alpha^2)^{1/2}}\right]^2\right)^{-1/2} m_e c^2, \qquad (3)$$

are nearly equal in the two cases. Nevertheless, there remains a large difference between the QED contributions to the transition energies because these contributions have a faster Z scaling than the Dirac contributions. For the example given, the energy difference between $2p_{3/2} - 1s_{1/2}$ (Mn^{24+}) and $3p_{3/2} - 1s_{1/2}$ (V^{22+}) is 2.9 eV, of which the difference between the $1s$ Lamb shifts in the two ions accounts for 0.9 eV. Therefore, such a measurement scheme is sensitive to the small, uncertain part that is of interest, and insensitive to the large Dirac part, which is already known exactly. The interval of interest can be calibrated by the two fine-structure intervals which appear automatically in the measurement and are very well known from theory. A determination of the line centroids to 1 part per million would result in a measurement of the difference in ground state Lamb shifts between the two ions to a precision of 0.7%, significantly better than any direct 1s Lamb shift measurement to date. Work in this direction has begun at the Oxford EBIT using the instrumentation described above. We have made a first observation of the Lyman-β lines of V^{22+}.

5 Conclusions

The use of a Johann-type curved crystal spectrometer and an electron beam ion trap allow us to obtain X-ray specta of the Lyman-α lines of medium Z

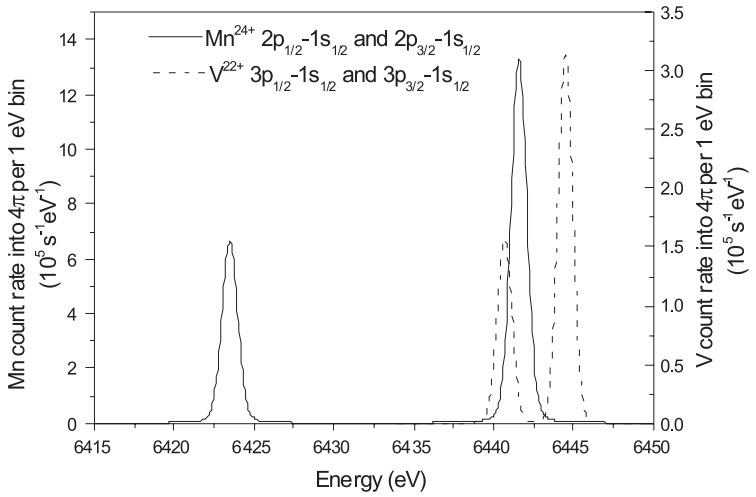

Fig. 6. A simulation of the lines to be expected in the intercomparison of Mn^{24+} Lyman-α and V^{22+} Lyman-β

hydrogen-like ions with high resolution and high statistical precision. The calibration of such spectra to the same level of precision remains problematic, but might be achieved using standard Kα sources outside the EBIT. An intercomparison method has been presented whereby QED effects in the ground states of hydrogen-like ions can be measured without any absolute calibration of the X-ray wavelengths. We acknowledge the support of the Japanese Science and Technology Corporation, useful discussions with C. Chantler, the technical expertise of P. Hirst, T. Handford, K. Kiley and K. Schaub, and the extremely valuable support given by R. Barnsley, N. Nelms, N. Peacock and staff at UKAEA-Culham.

References

1. K. Pachucki, D. Leibfried, M. Weitz, A. Huber, W König, T. W. Hänsch: J. Phys. B **29**, 177 (1996)
2. M. I. Eides, V. A. Shelyuto: Phys. Rev. A **52**, 954 (1995)
3. S. Mallampalli, J. Sapirstein: Phys. Rev. Lett. **80**, 5297 (1998)
4. I. Goidenko, L. Labzowsky, A. Nefiodov: Phys. Rev. Lett. **83**, 2312 (1999)
5. R. Pohl et al.: *this edition*, pp. 454–466
6. W. R. Johnson, G. Soff: Atomic Data Nucl. Data Tables **33**, 405 (1985)
7. C. Schwob et al.: Phys. Rev. Lett. **82**, 4960 (1999)
8. H. F. Beyer, R. D. Deslattes, F. Folkmann, R. E. LaVilla: J. Phys. B **18**, 207 (1985)
9. H. F. Beyer, P. Indelicato, K. D. Finlayson, D. Liesen, R. D. Deslattes: Phys. Rev. A **43**, 223 (1991)
10. M. Tavernier, J. P. Briand, P. Indelicato, D. Liesen, P. Richard: J. Phys. B **18**, L327 (1985)
11. J. P. Briand, P. Indelicato, A. Simionovici, V. San Vincente, D. Liesen, D. Dietrich: Europhys Lett **9**, 225 (1989)

12. H. F. Beyer et al.: Z. Phys. D **35**, 169 (1995)
13. Th. Stöhlkler: presented at the conference *Hydrogen Atom 2* (unpublished)
14. G. Hölzer et al.: Phys. Rev. A **57**, 945 (1998)
15. H. Johann: Z. Phys. **69**, 185 (1931)
16. J. D. Silver et al.: Rev. Sci. Instrum. **65**, 1072 (1994)
17. M. A. Levine, R. E. Marrs, J. R. Henderson, D. A. Knapp, M. B. Schneider: Physica Scripta. **T22**, 157 (1988)
18. P. Beiersdorfer, A. L. Osterheld, V. Decaux, K. Widmann: Phys. Rev. Lett **77**, 5353 (1996)
19. P. Beiersdorfer, J. R. Crespo López-Urrutia, E. Förster, J. Mahiri, K. Widmann: Rev. Sci. Instrum. **68**, 1077 (1997)
20. C. T. Chantler: private communication (2000)
21. C. T. Chantler: J. Appl. Cryst. **25**, 674 (1992)
22. J. R. Crespo López-Urrutia, B. Bapat, J. Ullrich: "Spectroscopy of Few-Electron, Highly Charged Ions with the Freiburg Electron Beam Ion Trap FreEBIT". Presented at ICAP, Florence, June 4-9, 2000; Book of abstracts, p.178
23. P. Indelicato et al.: presented at the conference *Hydrogen Atom 2* (unpublished)